KURTOSIS DPLL AND PTCM DECODER FOR NON-LINEARLY AMPLIFIED 16-QAM

S. Jayasimha and P. Jyothendar
Signion Systems Ltd.
Hyderabad, India

ABSTRACT

We describe a non-decision directed kurtosis-based digital phase lock loop (DPLL) algorithm for 16-QAM carrier recovery in the presence of non-linear amplification. A constellation rotation (with respect to locked phase) allows each of the trellis decoder's set-partitions to be fully confined to the received vector quadrants. Transponder characteristic variations may be automatically tracked by adapting the TCM decoder's metric LUT based on 4 dominant maxima in a 2-D histogram of quadrant data.

INTRODUCTION

Operated near saturation from efficiency considerations, satellite transponder distortion of a high-order modulation (HOM) degrades performance of a receiver that presumes an undistorted constellation. For example, satcom standards such as [1, 2] use 16-QAM modulation (see Figure 1) together with inner pragmatic trellis coded modulation (PTCM), relying on an "industry standard" constraint length 7, rate ½, convolutional code, and a Reed-Solomon outer code over GF(2^8).

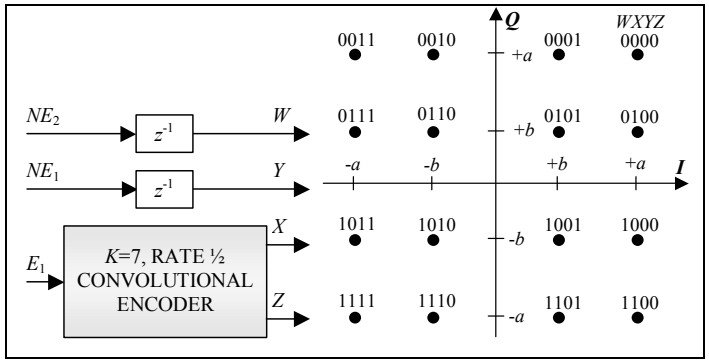

Figure 1. 16-QAM PTCM and constellation mapping (not $n\cdot\pi/2$ rotationally invariant)

For a general 16-QAM, the constellation points $I+jQ$ allow $I=\pm a, \pm b$, $Q=\pm a, \pm b$, yielding a signal power, $S=a^2+b^2$ and three possible IF signal amplitudes: $\sqrt{2}\cdot b$, $(a^2+b^2)^{0.5}$ and $\sqrt{2}\cdot a$. With an unequally-spaced constellation, e.g., $a=\pm\cos(\pi/8)$ and $b=\pm\sin(\pi/8)$, the peak-to-rms ratio of carrier-modulated 16-QAM is $2\cdot a\cdot(a^2+b^2)^{-0.5}=2\cdot\cos(\pi/8)$ (i.e., 5.33dB at carrier; 2.33dB at baseband).

Two methods of mitigating non-linear amplification effects of satellite transponders on HOMs are:

- Transmit-side pre-distortion [3,4], requiring prior knowledge of satellite transponder characteristics (that are presumed predictable with respect to operating temperature and aging)
- Receive-side mitigation techniques include, among others, equalization based on a Volterra expansion of the non-linear channel [5,6] and decision feedback [7]

We describe two variations to [7]'s receive-side mitigation, that improve 16-QAM TCM decoder performance in the presence of:

- Recovered carrier phase noise
- Non-linear phase (w.r.t. frequency) response of analog (e.g., low insertion loss SAW) filters
- Varying (e.g., w.r.t. temperature and age) non-linear power amplifier phase and amplitude response.

In this paper's next section, [7]'s TCM decoder based decision-directed[1] phase/ amplitude vector tracker is omitted[2] in favor of low-complexity, non-decision directed kurtosis computations (briefly described in [8]) that allow the receiver's DPLL to adapt automatically (and independent of TCM decoder) to the transponder's (potentially varying) input amplitude-dependent phase and amplitude responses. Prior work on blind QAM carrier phase tracking, either for dispersive channels [9], or additive-noise, non-dispersive channels (raising received data to the 4th power and then determining concentration ellipse orientation) [10], have not been extended to the memory-less non-linear satellite channel.

In the subsequent section, maximum likelihood (ML) vectors, for each of the three 16-QAM constellation's amplitudes, are recovered from four dominant peaks in a 2-D histogram of received vectors (each rotated into the first quadrant) in order to update the trellis decoder's metric

[1] A decision-directed PLL's (DDPLL's) initial convergence rate depends upon the deviation of the actual transponder's characteristic from an initially presumed default (which is updated as the system learns); a non-decision directed approach achieves rapid phase-lock without making any assumptions on transponder AM-AM or AM-PM response.

[2] It may be advantageous, e.g., with more advanced coding schemes, to take a combined approach where a kurtosis DPLL is used during acquisition and the decision-directed approach of [7] during tracking.

look-up table (LUT), reducing, when compared to the sub-domain centroids method of [7], centrifugal displacement, at low SNR, of the four estimated vectors from the actual transmit vectors.

Experimental results and conclusions are provided in the paper's final sections.

NON DECISION-DIRECTED DPLL FOR NON-LINEARLY AMPLIFIED 16-QAM

A non decision-directed DPLL for undistorted16-QAM (of Figure 1) may be based on the phase dependence of kurtosis of either channel (say, Q), with $S=a^2+b^2$ and $\rho=b/a$, $\kappa=[\rho/(1+\rho^2)]^2$ according to (with A=1.875 and B=0.375 for no-noise[3] case):

$$\frac{E[(Q')^4]}{E[(Q')^2]^2}=\left[\frac{9}{4}+3\cdot\kappa\cdot\left(\frac{2N}{S}-1\right)\right]-\left[\left(\frac{1}{4}+\kappa\right)\cdot\left(1-\frac{2N}{S}\right)\right]\cdot\cos[4(\phi+\psi)]$$
$$=A\text{-}B\cdot\cos[4(\phi+\psi)] \qquad (1)$$

A band-limited, reduced peak-to-rms, 16-QAM modulation is achieved either by pulse shaping a pre-distorted constellation or by RF bandlimiting of non-linearly amplified 16-QAM signal (avoiding spectral regrowth beyond a stipulated spectral mask). For a TWTA, the Saleh model [11] baseband amplitude (AM-AM) and phase (AM-PM) responses are $A(r)=\alpha_a\cdot r/(1+\beta_a\cdot r^2)$ and $\phi(r)=\alpha_\phi\cdot r^2/(1+\beta_\phi\cdot r^2)$ respectively as shown in Figure 2. Typical parameter values are α_a=2.0, β_a=1.0, α_ϕ=2.5 and β_ϕ=2.8.

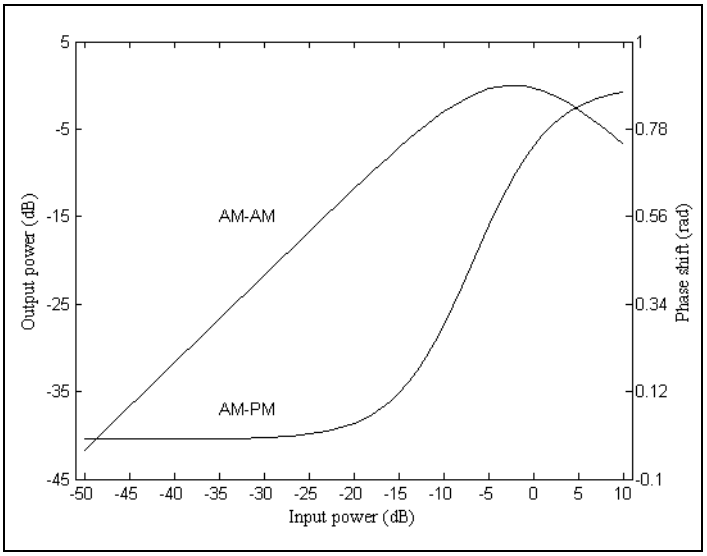

Figure 2. Typical TWTA AM-AM and AM-PM model

For GaAsFETs, the Ghorbani [12] model for AM-AM distortion, with $A(r)=[(x_1\cdot r^{x_2})/(1+x_3\cdot r^{x_2})]+x_4\cdot r$, may be used while Saleh's AM-PM distortion retained to obtain a 6 (rather than Ghorbani's 8) parameter model. Typical parameters are x_1=8, x_2=1.5, x_3=6.5, x_4=-0.1, α_ϕ=5.5 and β_ϕ=13. The AM-AM for SSPA [13] model is $A(r)=r/[1+r/(\alpha_a)]^{0.5}$ while $\phi(r)=0$, with α_a=0.4. Figure 3 shows the kurtosis vs. phase relationship for typical SSPA, TWTA and GaAsFET amplifier characteristics, which is of the form A-$B\cdot\cos[4(\phi+\psi)]$, where ψ, a phase offset, aligns all sub-constellations' centroids with the ±45° axes.

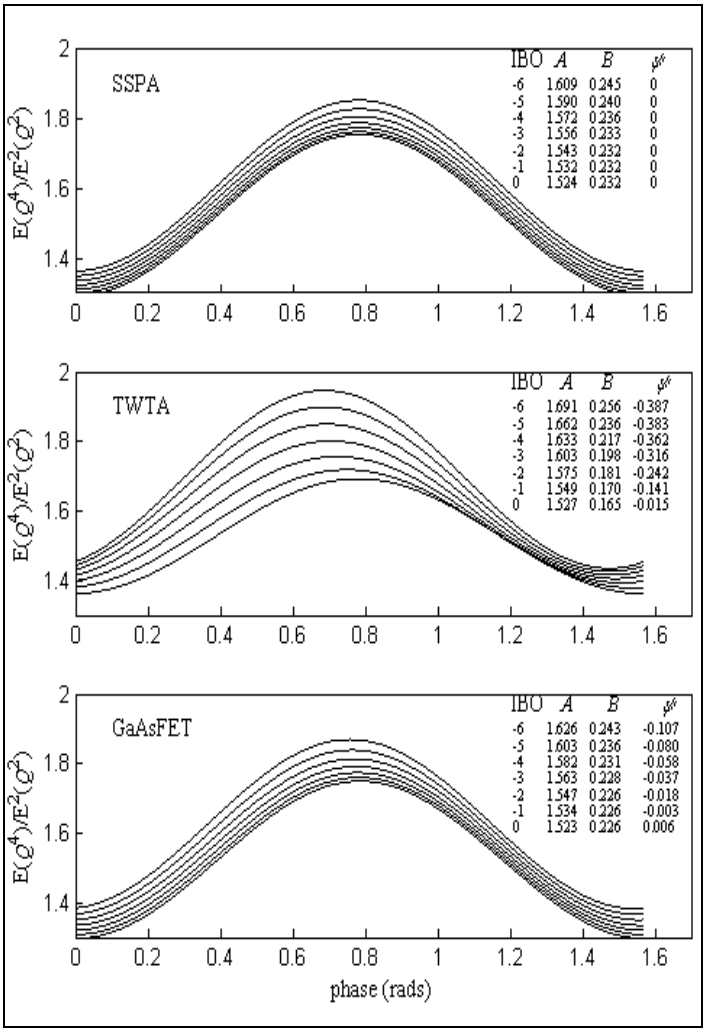

Figure 3. Kurtosis as a function of phase for typical SSPA, TWTA and GaAsFET amplifiers

$E[R^4]/E^2[R^2]=\{E[Q^4]+E[I^2Q^2]\}/\{2\cdot E^2[Q^2]\}$ determines[4] A. Irrespective of distortion, phase can be locked near ϕ=-

[3] 16-QAM TCM with outer Reed-Solomon coding (as per [1]), at operating SNR, has $2\cdot N/S\approx 0.08$; i.e., the high-backoff bias of A, due to neglecting (1)'s SNR dependence, is only 1% of its no-noise value.

[4] $$\frac{E(I^2\cdot Q^2)}{E^2(Q^2)}=\left[\frac{3}{4}+\kappa\cdot\left(\frac{2\cdot N}{S}-1\right)+\frac{N}{2\cdot S}\right]+\left[\left(\frac{1}{4}+\kappa\right)\cdot\left(1-\frac{2\cdot N}{S}\right)\right]\cdot\cos[4(\phi+\psi)]$$
$$=\frac{A}{3}-B\cdot\cos[4(\phi+\psi)]$$
e.g., A, computed as $1.5\cdot E[R^4]/E^2[R^2]$, has a high-backoff bias of $0.375\cdot(N/S)$ (≈0.8% of (1)'s 1st term value at a 14dB operating SNR).

$\pi/8$[5] using Figure 4's DPLL structure[6]. A kurtosis-based DPLL, while requiring the same AGC (and kurtosis) settling time as a DDPLL, has the following advantages:

- A kurtosis-based DPLL can achieve rapid phase-lock without making symbol decisions as opposed to a DDPLL that slowly adapts it decision boundaries to an unknown transmit back-off
- A block kurtosis estimate reuses partial block computations of other modules (e.g., AGC)

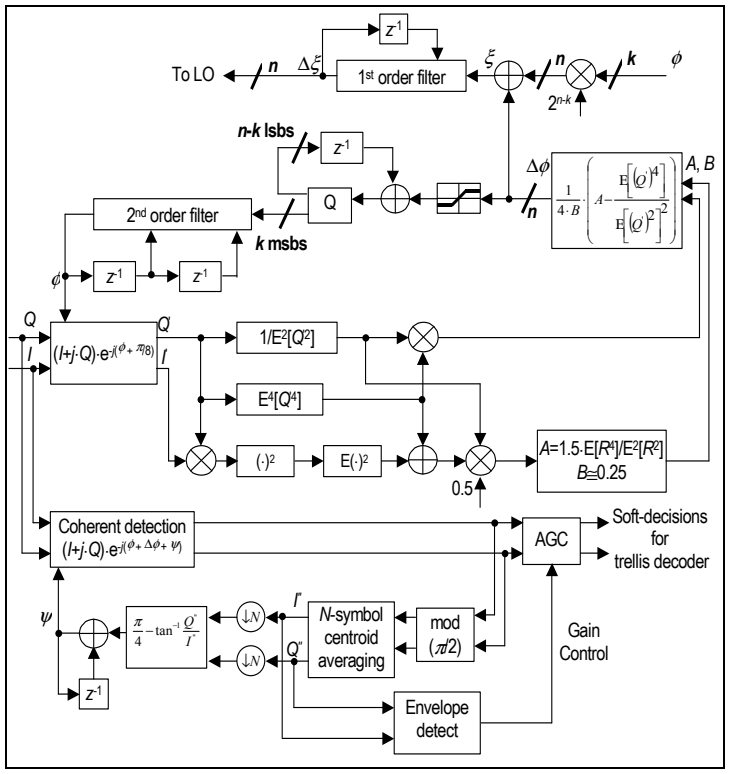

Figure 4. Kurtosis DPLL for 16-QAM; $n > k$

Even after the kurtosis-based DPLL is locked, a phase offset (with respect to aligning sub-constellations' centroids to the ±45° axes), ψ, exists due to the non-linear amplifier's AM/PM characteristic (as Figure 5 shows); ψ, computed as the difference between $\pi/4$ and the averaged centroids' argument[7] (modulo 90°), corrects this phase offset (together with any residual DPLL phase offset).

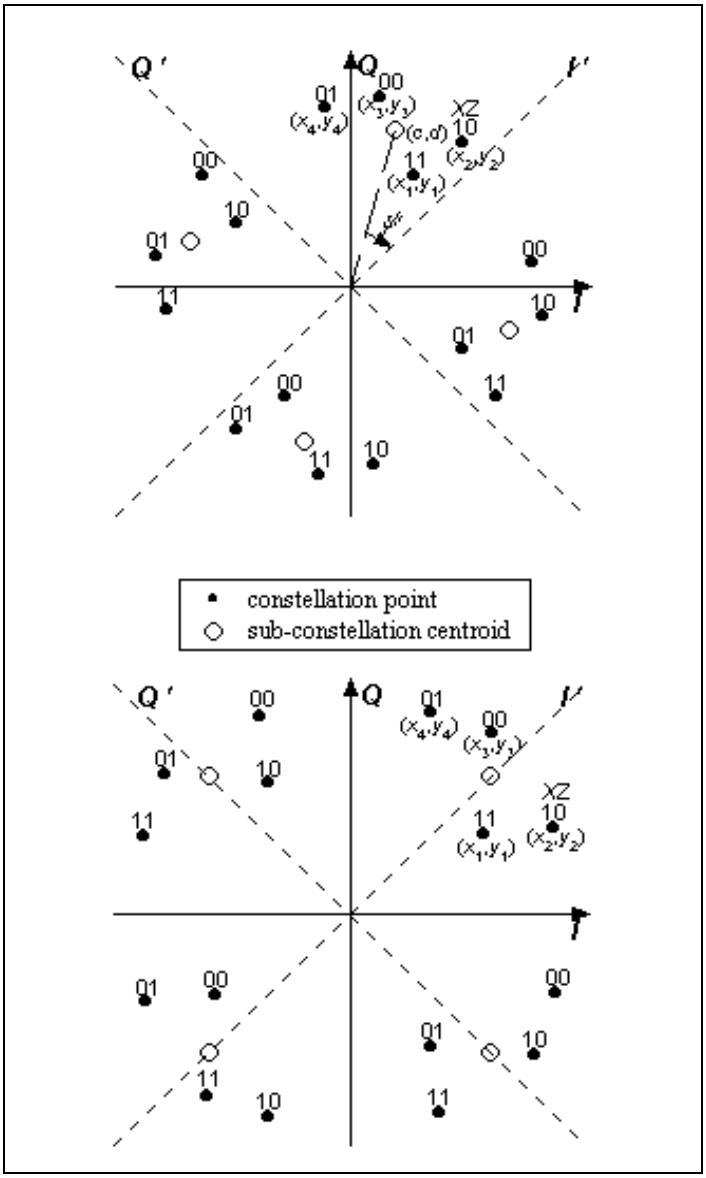

Figure 5. 16-QAM phase recovery (top) and rotated constellation presented to trellis decoder (bottom)

The AGC, initially controlled (as for constant envelope modulations) by $S+N$, is controlled by the averaged centroid modulus after phase lock, in order that the gain-

[5] When A is presumed (as a default on power-on, as the previous value otherwise) in burst mode, phase variations w.r.t. IBO are smaller at $-\pi/8$ (as compared to $\pi/8$).

[6] Using a smaller than true value for B increases DPLL phase noise, while selecting a larger B, such as 0.25 (see Figure 4), may result in a residual phase offset; however, this phase offset gets included in ψ.

[7] From Figure 5, $(x_1, y_1) = \left(\frac{\sqrt{2} \cdot b \cdot \alpha_a}{1 + 2 \cdot b^2 \cdot \beta_a} \right) \cdot e^{j\left[\frac{\pi}{4} + \frac{2 \cdot b^2 \cdot \alpha_\phi}{1 + 2 \cdot b^2 \cdot \beta_\phi} \right]}$

$$(x_2, y_2) = \left(\frac{\alpha_a \cdot \sqrt{a^2 + b^2}}{1 + \left(a^2 + b^2\right) \cdot \beta_a} \right) \cdot e^{j\left[\tan^{-1}\left(\frac{b}{a}\right) + \frac{\alpha_\phi \left(a^2 + b^2\right)}{1 + \left(a^2 + b^2\right) \beta_\phi} \right]}$$

$$(x_3, y_3) = \left(\frac{\sqrt{2} \cdot a \cdot \alpha_a}{1 + 2 \cdot a^2 \cdot \beta_a} \right) \cdot e^{j\left[\frac{\pi}{4} + \frac{2 \cdot a^2 \cdot \alpha_\phi}{1 + 2 \cdot a^2 \cdot \beta_\phi} \right]}$$

$$(x_4, y_4) = \left(\frac{\alpha_a \cdot \sqrt{a^2 + b^2}}{1 + \beta_a \cdot \left(a^2 + b^2\right)} \right) \cdot e^{j\left[\tan^{-1}\left(\frac{a}{b}\right) + \frac{\alpha_\phi \left(a^2 + b^2\right)}{1 + \beta_\phi \cdot \left(a^2 + b^2\right)} \right]}$$

Thus, the centroid $(c,d) = 0.25 \cdot (x_1+x_2+x_3+x_4\ ,\ y_1+y_2+y_3+y_4)$

compensated sub-constellations' centroids have a constant modulus at the trellis decoder's input.

16-QAM PTCM DECODING

Without distortion, each 16-QAM PTCM symbol is decoded, producing 3 bits per symbol, using very few additional computations over the underlying rate ½, constraint length 7, Viterbi decoder. We retain a low-complexity decoder for non-linearly amplified 16-QAM as well.

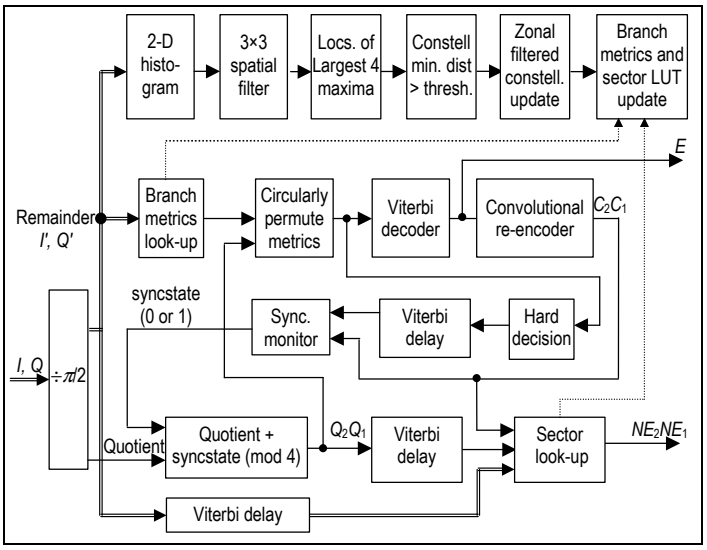

Figure 6. 16-QAM-Trellis decoder block diagram

In Figure 6, received I/Q vectors are rotated by $m\cdot\pi/2$, $m=\lfloor 2\cdot\arg(I+jQ)/\pi \rfloor$, to obtain I'/Q' vectors, that address the 1st quadrant Viterbi branch metrics LUT. These metrics are then circularly permuted, based on m, prior to being fed to the Viterbi decoder. Comparing the mismatches in delayed hard decisions and convolutionally re-encoded Viterbi output with a threshold indicates the decoder's synchronization state (a 90º phase rotation allowing synchronization[8] in the event of failure). Finally, the 1st quadrant non-encoded bits, obtained by using I'/Q' to index the sector LUT, are re-mapped to the m-th quadrant. In parallel, branch-metric and sector LUTs are updated by finding 4 dominant maxima in a spatially filtered 2-D histogram, averaged over a suitable period, of I'/Q' vectors. Minimum intra-constellation distance thresholding and constellation change zonal filtering prevents the LUTs from ever being contaminated by erroneously estimated signal sets. Measured E_b/N_0 (with distortion) may be used to calibrate the E_b/N_0 estimate provided by the rate-3/4 16-QAM TCM decoder, which is based on all quadrants' 4-QAM hard-decision error rate[9].

EXPERIMENTAL RESULTS

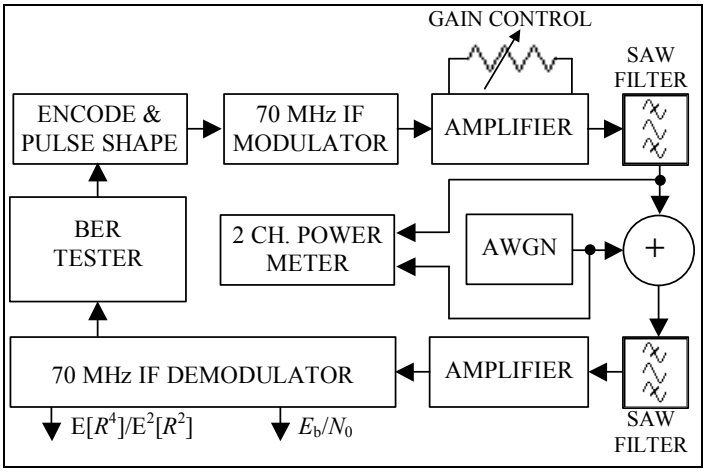

Figure 7. 16-QAM performance testing w.r.t. distortion

The set-up of Figure 7 measures distortion-adaptive demodulator performance. An attenuator sets the modulator amplifier's IBO, while the demodulator's $E[R^4]/E^2[R^2]$ infers IBO. Figure 8 shows unsaturated and saturated 16-QAM performance, each with its associated constellation. ML-derived constellations are not centrifugally displaced, while domain-derived centroids are.

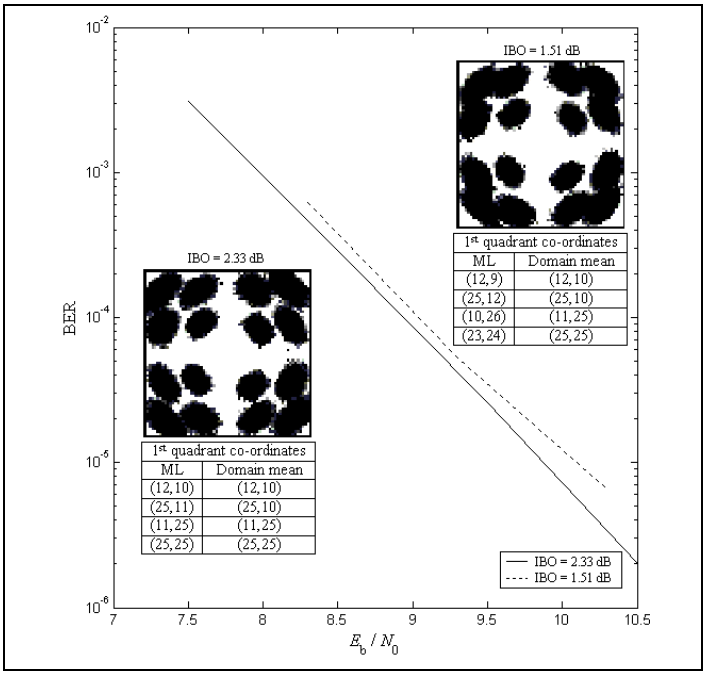

Figure 8. b/a=0.414 16-QAM performance with 2.33 and 1.51dB IBO's; symbol-time bandwidth product ($B\cdot T_s$)=1

[8] Unique-word based outer (e.g., Reed-Solomon) code frame synchronizer resolves 180° phase ambiguity

[9] For 4-QAM with $P_b \approx Q[(0.5\cdot d^2_{min}/N_0)^{0.5}] > 0.5\cdot erfc[(E_b/N_0)^{0.5}]$; at high SNR, $P_b > 0.25\exp[-0.5\cdot(E_b/N_0)]$. A correction (via calibration) to estimated E_b/N_0 (with distortion) is made because, in dB, $(E_b/N_0)_{4\text{-QAM}} > 10\cdot\log_{10}[-2\cdot\ln(4\cdot P_b)]$ and $(E_b/N_0)_{16\text{-QAM}} = 6.58 + (E_b/N_0)_{4\text{-QAM}}$.

CONCLUSIONS

Optimum 16-QAM demodulator performance on diverse satellite channels (e.g., using SSPA, TWTA, or GaAsFET power amplifiers) is obtained via:

- A robust and computationally efficient non-decision directed DPLL for fast phase and frequency acquisition
- Unambiguous subset (quadrant) partitioning/ labeling
- TCM decoder LUT update based on 4 dominant maxima in a 2-D histogram of quadrant data

While kurtosis DPLL expressions and constellation recovery remain identical for non-square (NS) 8-QAM [14], other (higher order) QAMs, as well as other codes (e.g., LDPC), can be processed with a similar methodology. Though the non-decision directed DPLL described here provides good performance for the particular 16-QAM/TCM considered, it may be advantageous to use non-decision directed DPLL during acquisition and the decision directed approach of [7] during tracking for other modulations and codes (e.g. [14]).

REFERENCES

[1] EN 301 210 *Digital Video Broadcasting* (DVB); Framing structure, channel coding and modulation for *Digital Satellite News Gathering* (DSNG) and other contribution applications by satellite, v1.1.1 (1999-03).

[2] *Intelsat Earth Station Standards* (IESS), Document IESS-316, Performance characteristics for digital carriers using 16-QAM modulation, October 24, 2003

[3] G. Karam and H. Sari, "Analysis of predistortion, equalization, and ISI cancellation techniques in digital radio systems with nonlinear transmit amplifiers," *IEEE Trans. Commun.*, vol. 37, pp. 1245-1252, December 1989.

[4] G. Karam and H. Sari, "A data predistortion technique with memory," *IEEE Trans. Commun.*, vol. 39, pp. 336-344, February 1991.

[5] S. Benedetto, E. Biglieri and R. Daffara, "Modeling and performance evaluation of nonlinear satellite links – a Volterra series approach," *IEEE Trans. Aerosp. Electron. Syst.*, vol. 15, pp. 494-507, July 1979.

[6] S. Benedetto and E. Biglieri, "Nonlinear equalization of digital satellite channels," *IEEE J. Select. Areas Commun.*, vol. 1, pp. 57-62, January 1983.

[7] R. De Gaudenzi and M. Luise, "Analysis and design of all-digital demodulator for trellis-coded 16-QAM transmission over a nonlinear satellite channel," *IEEE Trans. Commun.*, vol. COM-43, pp. 659-667, Feb.-Apr., 1995.

[8] S. Jayasimha, P. Jyothendar and S. Pavanalatha, "SDR Framework for burst/continuous MPSK/ 16-QAM modems," Proc. of *SPCOM '-04*, ISBN 0-7803-8675-2, IEEE catalog no. 04EX926C.

[9] A. Belouchrani and W. Ren, "Blind carrier phase tracking with guaranteed global convergence," *IEEE Trans. on Sig. Proc.*, vol. 45, pp. 1889-1894, July 1997.

[10] P. Campisi et. al, "Blind Phase Recovery for QAM Communication Systems," *IEEE Trans. on Sig. Proc.*, vol. 53, pp. 1348-1357, April 2005.

[11] A. A. M. Saleh, "Frequency-independent and frequency-dependent nonlinear models of TWT amplifiers," *IEEE Trans. Commun.*, vol. COM-29, pp. 1715-1720, November, 1981.

[12] A. Ghorbani and M. Sheikhan, "The effect of Solid State Power Amplifiers (SSPAs) Nonlinearities on MPSK and M-QAM Signal Transmission", *Sixth Int'l Conference on Digital Processing of Signals in Comm*., 1991, pp. 193-197.

[13] R. Nee and R. Prasad, *OFDM for Wireless Multimedia Communications*, Artech House Publishers, 2000.

[14] L. Li, D. Divsalar and S. Dolinar, "Iterative Demodulation, Demapping and Decoding of Coded Non-Square QAM," *IEEE Trans. Commun.*, vol. 53, pp. 16-19, Jan., 2005.